INVITED PAPER *Special Section on Recent Progress in Superconducting Analog Devices and Their Applications*

Liquid-Phase Detection of Biological Targets with Magnetic Marker and Superconducting Quantum Interference Device

Keiji ENPUKU[†a)], ***Member***, **Yuki SUGIMOTO**[†], **Yuya TAMAI**[†], **Akira TSUKAMOTO**[††], **Takako MIZOGUCHI**[††], ***Nonmembers***, **Akihiko KANDORI**[††], ***Member***, **Naoki USUKI**[†††], **Hisao KANZAKI**[†††], **Kohji YOSHINAGA**[††††], **Yoshinori SUGIURA**[†††††], **Hiroyuki KUMA**[†††††], ***and*** **Naotaka HAMASAKI**[††††††], ***Nonmembers***

SUMMARY Liquid-phase detection of biological targets utilizing magnetic marker and superconducting quantum interference device (SQUID) magnetometer is shown. In this method, magnetic markers are coupled to the biological targets, and the binding reaction between them is detected by measuring the magnetic signal from the bound markers. Detection can be done in the liquid phase, i.e., we can detect only the bound markers even in the presence of unbound (free) markers. Since the detection principle is based on the different magnetic properties between the free and bound markers, we clarified the Brownian relaxation of the free markers and the Neel relaxation of the bound markers. Usefulness of the present method is demonstrated from the detection of the biological targets, such as biotin-coated polymer beads, IgE and *Candida albicans*.

key words: *liquid-phase immunoassay, magnetic marker, Brownian relaxation, Neel relaxation, B/F separation, SQUID*

1. Introduction

Recently, magnetic immunoassays utilizing magnetic markers have been developed to detect biological targets [1]–[11]. In this method, the magnetic marker is made of magnetic nanoparticles coated with detecting antibodies. The magnetic marker selectively couples to the biological target, and the binding reaction between the target and the marker is detected by measuring the magnetic signal from the bound markers.

One of the merits of the magnetic method is that we can perform immunoassay in the liquid phase, i.e., we can detect only the bound markers even in the presence of unbound (free) markers without using the so-called bound/free (BF) separation process. We can distinguish the bound markers from the free ones by utilizing the difference in the magnetic properties between them. This function has been demonstrated using relaxation or susceptibility measurement of the markers in solution [3]–[11]. Since time-consuming process of the BF separation can be eliminated, we can expect a high-speed immunoassay with the magnetic method.

Magnetic properties of the free markers are dominated by the Brownian relaxation in solution. On the other hand, magnetic properties of the bound markers are dominated by the Neel relaxation. It is well known, however, that these magnetic relaxations strongly depend on various parameters of the marker, such as marker size, size distribution of the marker and the degree of aggregation of the markers [12]–[14]. Since these effects are significant in practical samples, it is important to clarify the magnetic properties of practical samples by taking account of these effects.

In this paper, we first show the magnetic properties of the marker. The Brownian relaxation of the free markers is studied from the frequency dependence of the susceptibility in solution. Analyzing the frequency dependence with the mathematical technique called singular value decomposition (SVD) method, we estimate the distribution of the marker size. The Neel relaxation of the bound markers is also studied. Next, we show detection system for the liquid-phase immunoassay, which is based on the different magnetic relaxations between the bound and free markers. Using this system, we conduct the detection of biological targets, such as biotin-coated polymer beads, IgE and *Candida albicans*, and show the usefulness of the present method.

2. Magnetic Properties of the Marker

2.1 Magnetic Marker

The magnetic markers were made of Fe_3O_4 particle coated with polymer. Since the markers are under development, we show an example of the markers. Transmission electron microscopy (TEM) image of the Fe_3O_4/polymer particle is shown in Fig. 1. As shown, size of single Fe_3O_4 particle was typically 20–25 nm. It was difficult to observe the polymer coating, which means that the thickness of the polymer coating was very thin compared to the Fe_3O_4 particle.

Magnetization curve of the Fe_3O_4/polymer particle was measured with vibrating sample magnetometer (VSM). The measurement was done using a powder of the Fe_3O_4/polymer particles. We obtained the saturation magnetization $\mu_0 M_s$ = 460 mT and the remanence $\mu_0 M_r$ =

Manuscript received June 27, 2008.
Manuscript revised August 31, 2008.

[†]The authors are with Research Institute of Superconductor Science and Systems, Kyushu University, Fukuoka-shi, 819-0395 Japan.
[††]The authors are with Advanced Research Laboratory, Hitachi Ltd., Kokubunji-shi, 185-8601 Japan.
[†††]The authors are with R and D Division, Hitachi Maxell Ltd., Kyoto-fu, 618-8525 Japan.
[††††]The author is with the Department of Applied Chemistry, Kyushu Institute of Technology, Kitakyushu-shi, 804-8550 Japan.
[†††††]The author is with Plastic Products Division, INOAC Corporation, Nagoya-shi, 456-0054 Japan.
[††††††]The authors are with the Faculty of Pharmaceutical Sciences, Nagasaki International University, Sasebo-shi, 859-3298 Japan.
a) E-mail: enpuku@sc.kyushu-u.ac.jp
DOI: 10.1587/transele.E92.C.315

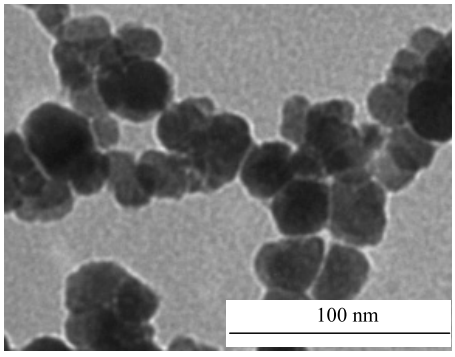

Fig. 1 TEM image of the Fe_3O_4 particles. Typical particle size was 20–25 nm. The aggregated structure of the particles was caused when the particles in liquid was dried for TEM measurement.

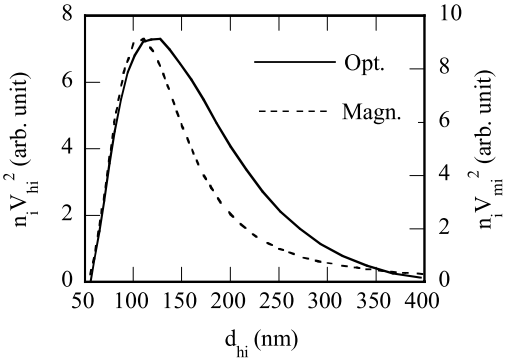

Fig. 2 Size distribution of the magnetic marker in pure water. The solid line shows the d_{hi}-$n_i V_{hi}^2$ curve obtained from the optical measurement (DLS). The broken line shows the d_{hi}-$n_i V_{mi}^2$ curve that was obtained by analyzing the frequency dependence of the susceptibility shown in Fig. 3 with the SVD method.

32 mT. The apparent coercive field that produced $M = 0$ was 2.6 mT.

Magnetic marker was made by coating avidin to the Fe_3O_4/polymer particle, i.e., avidin-coated Fe_3O_4/polymer particles. The size distribution of the magnetic marker in pure water was measured with dynamic light scattering (DLS). The result is shown in Fig. 2 by the solid line. The horizontal axis is the hydrodynamic diameter d_{hi}, while the vertical axis on the left represents the distribution of $n_i V_{hi}^2$. Here n_i and $V_{hi} = (\pi/6)d_{hi}^3$ are the number and the hydrodynamic volume of the i-th marker, respectively. As shown, the diameter d_{hi} of the marker distributed in the range from 50 nm to 400 nm. Typical value of the diameter, which gave the peak of $n_i V_{hi}^2$, was $d_{hi} = 120$ nm.

We note that the size of the single Fe_3O_4 particle was typically 20–25 nm as shown in Fig. 1. Compared to this value, the size of the marker is very large. This difference indicates that aggregation of the Fe_3O_4 particles occurred in making magnetic markers, i.e., the marker consists of aggregated Fe_3O_4 particles. Therefore, magnetic properties of the marker correspond to those of the aggregated Fe_3O_4 particles.

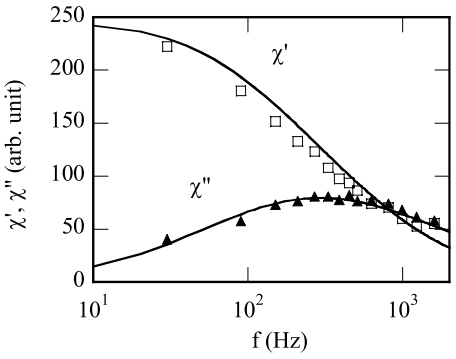

Fig. 3 Frequency dependence of the susceptibility of the magnetic marker in solution. The open and closed symbols represent the real and imaginary part of the susceptibility, respectively. The solid lines show the analytical results calculated from Eqs. (1) and (2) with the d_{hi}-$n_i V_{mi}^2$ curve shown by the broken line in Fig. 2.

2.2 Brownian Relaxation of Free Markers

First, we study the Brownian relaxation of the free markers. For this purpose, we measured ac susceptibility of the magnetic marker in solution, since the susceptibility shows the frequency dependence characterized by the Brownian rotation of the magnetic marker. When we take account of the size distribution of the magnetic marker, the real and imaginary parts of the susceptibility, i.e., χ' and χ'', are given by [12].

$$\chi'(\omega) = \frac{\mu_0 M_s^2}{3k_B T V_T} \sum_i \frac{n_i V_{mi}^2}{1 + (\omega\tau_i)^2} + \chi_\infty \tag{1}$$

$$\chi''(\omega) = \frac{\mu_0 M_s^2}{3k_B T V_T} \sum_i \frac{\omega\tau_i n_i V_{mi}^2}{1 + (\omega\tau_i)^2} \tag{2}$$

where $V_T = \sum n_i V_{mi}$ is the total volume of the sample, and χ_∞ represents the susceptibility at high frequency limit. The value V_{mi} represents the magnetic volume of the i-th marker.

The relaxation time τ_i of the Brownian rotation of the marker is given by

$$\tau_i = 3\eta V_{hi}/k_B T \tag{3}$$

where η is the viscosity of the carrier liquid, k_B is the Boltzmann constant and T is the absolute temperature. In the present case $\eta = 10^{-3}$ kg/ms for water, and $T = 300$ K.

In the experiment, 5 μg of the markers were diluted in 50 μl pure water. Susceptibility of this sample was measured with magneto-resistance (MR) sensor by applying an external ac field of $\mu_0 H = 200\,\mu$T. In Fig. 3, the frequency dependence of the susceptibility is shown. The vertical axis represents the value of the susceptibility in arbitrary unit. Open and closed symbols represent the real and imaginary part of the susceptibility, respectively. As shown, the real part χ' decreased monotonically with the frequency, while the imaginary part χ'' had a broad peak around the frequency $f = 380$ Hz.

From Eq. (2), we can see that the peak of χ'' occurs

at the frequency $f = 1/(2\pi\tau_i)$. Therefore, typical relaxation time corresponding to $f = 380\,\mathrm{Hz}$ becomes $\tau_i = 0.42\,\mathrm{ms}$. Using this value and Eq. (3), we obtain the typical hydrodynamic diameter of the marker as $d_{hi} = 110\,\mathrm{nm}$. This value is in good agreement with the typical value of $d_{hi} = 120\,\mathrm{nm}$ measured with DLS, which is shown in Fig. 2.

Analyzing the frequency dependence of the susceptibility shown in Fig. 3, we can estimate the size distribution of the marker. For this purpose, we used the mathematical technique called singular value decomposition (SVD) method. Details of the SVD method were described in Refs. [15] and [16]. The estimated size distribution, i.e., d_{hi}-$n_i V_{mi}^2$ curve, is shown in Fig. 2 by the broken line. We can compare the size distribution obtained from the magnetic measurement (SVD) and the optical measurement (DLS). Here, we can assume $V_{hi} = V_{mi}$ since the thickness of the coating material is very thin compared to the diameter of the Fe_3O_4 particle. As shown, size distributions estimated from the two measurements reasonably agree with each other.

Using the estimated size distribution shown in Fig. 2, i.e., d_{hi}-$n_i V_{mi}^2$ curve, we reconstructed the frequency dependence of the susceptibility from Eqs. (1) and (2). The solid lines in Fig. 3 represent the results. As shown, good agreements were obtained between the calculated results and the experimental ones. This agreement also indicates the validity of the size distribution estimated with the magnetic method.

We note that the diameter d_{hi} of the marker distributed in the range $50\,\mathrm{nm} < d_{hi} < 400\,\mathrm{nm}$ as shown in Fig. 2. From Eq. (3), therefore, we can estimate that the Brownian relaxation time of the free markers distributes in the range of $47\,\mu\mathrm{s} < \tau_i < 24\,\mathrm{ms}$.

2.3 Neel Relaxation of Bound Markers

Next, we measured the Neel relaxation of the magnetic marker, since it determines the magnetic properties of the bound markers. For this purpose, the magnetic marker in pure water was frozen. In this case, the Brownian rotation of the marker is prevented, and relaxation of magnetization is caused by the Neel relaxation of the Fe_3O_4 particles. The decay of magnetization M after the external field is turned off is given by [16]

$$M(t) = \sum_i M_i \exp(-t/\tau_{Ni}) \tag{4}$$

where τ_{Ni} and M_i are the Neel relaxation time and the magnetization of the i-th marker, respectively.

In the experiment, the external field of $\mu_0 H = 60\,\mathrm{mT}$ was applied to the frozen sample, and then turned off. Relaxation of magnetization M of the sample was measured with the SQUID sensor. The result is shown in Fig. 4 by open circles.

Analyzing the decay of M, we can estimate typical Neel relaxation times of the sample. For this purpose, we fit the experimental data with the so-called successive reduction method [16]. We obtained two typical sets (M_i, τ_{Ni}) = (419, 3.8 s) and (119, 87.1 s). The solid line in Fig. 4 shows the analytical result calculated with these parameters. As shown, the calculated result agrees well with the experiment. We note, however, that the Neel relaxation time depends on the temperature T as $\tau_N = \tau_0 \exp(KV/k_B T)$. Therefore, strictly speaking, the Neel relaxation time of the particles in liquid ($T = 300\,\mathrm{K}$) is a little faster than that measured in the frozen sample ($T = 273\,\mathrm{K}$).

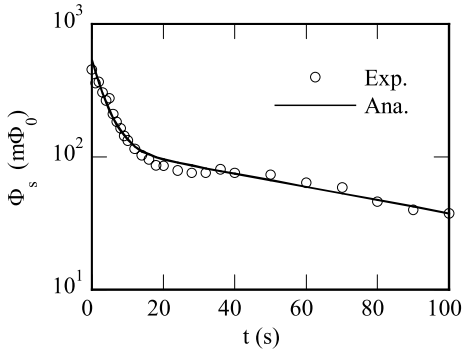

Fig. 4 Relaxation of magnetization M when the magnetic marker in water was frozen. Symbols show the experimental result of Neel relaxation, while the solid line represents the analytical result calculated from Eq. (4) with parameters (M_i, τ_{Ni}) = (419, 3.8 s) and (119, 87.1 s).

As mentioned in Sect. 2.2, the Brownian relaxation times of the free markers distribute in the range of $47\,\mu\mathrm{s} < \tau_i < 24\,\mathrm{ms}$. The Neel relaxation times of the bound markers, i.e., $\tau_{Ni} = 3.8$ and 87.1 s, are much longer than the Brownian relaxation times of the free markers. This difference can be used in performing the liquid phase immunoassay, as will be shown in the next section.

3. Principle of Liquid Phase Immunoassay

In Fig. 5, measurement process of the conventional solid phase immunoassay is schematically shown. The experimental procedures are as follow. First, (a) capturing antibodies are fixed on the base of the reaction chamber, and then (b) biological targets (antigens) are coupled to the capturing antibodies. Next, (c) magnetic markers coated with detecting antibodies are put into the reaction chamber. In this case, some of the markers are bound to the targets, but others remain unbound (free). In order to separate the bound markers from the free ones, (d) the free markers are washed out. This washing process is called bound/free (BF) separation. Then, (e) we can obtain the sample for the measurement. As shown above, we need a lot of sample-preparation procedures before measurement. Due to the time consuming process, it is difficult to realize a high-speed detection.

In order to realize a high-speed immunoassay, we developed a liquid phase immunoassay as shown below. In Fig. 6(a), measurement method is schematically shown. In the present method, antigens are fixed on the surface of large polymer beads with diameter $d_p = 3.3\,\mu\mathrm{m}$, instead of the base of the reaction chamber. When the magnetic markers are put into the solution, bound and free markers co-exist as

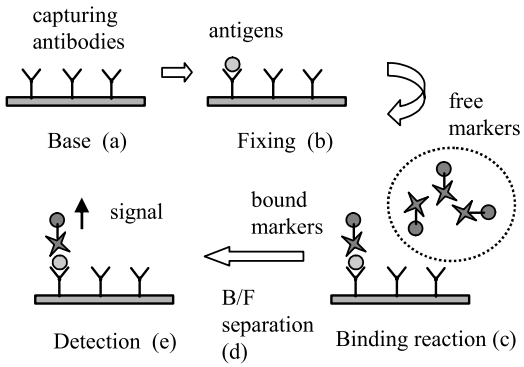

Fig. 5 Measurement process of the conventional solid phase immunoassay.

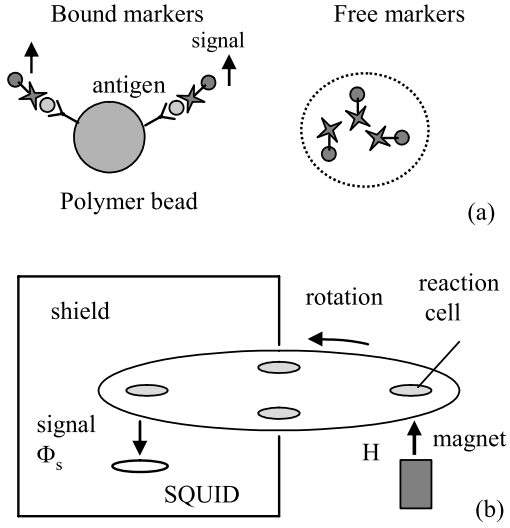

Fig. 6 (a) Detection principle of liquid phase immunoassay using polymer beads. (b) Schematic figure of the detection system.

shown in Fig. 6(a).

The bound markers are distinguished from the free ones by using the difference in the magnetic relaxation between them. In Fig. 6(b), the measurement process is schematically shown. As shown, there are three steps, i.e., (a) magnetization, (b) relaxation, and (c) detection. First, the samples are magnetized by an external small magnet. In this magnetization step, magnetic moments of both the bound and free markers are aligned to the direction of the external filed. Next, the reaction cell is rotated, and the external field becomes zero. In this relaxation step, the Brownian rotation of the free markers begins to occur, and the directions of the magnetic moments tend to be random. Since the relaxation time of the free markers is typically $\tau_i = 0.4$ ms as shown in Sect. 2.2, the magnetic signal from the free markers rapidly decay to zero.

On the other hand, the Brownian rotation of the bound markers is determined by the polymer beads. Due to the large diameter of the polymer bead $d_p = 3.3\,\mu$m, the relaxation time becomes as long as $\tau_{Bp} = 14$ s. This means that the Brownian relaxation of the bound markers becomes negligible compared to that of the free markers. Although Neel relaxation occurs in the bound markers, its relaxation time is also long, i.e., $\tau_N > 3.8$ s as shown in Sect. 2.3.

The waiting time T_w between the magnetization and the detection is set as $T_w = 1$ s in the present case. During this waiting time, the signal from the free markers decays to zero. On the other hand, signal from the bound markers is kept constant, and can be measured with the SQUID system [17]. Therefore, we can detect only the signal from the bound markers even in the presence of the free markers.

As shown in Fig. 6(a), many antigens are fixed to one polymer bead. We note that we do not need to precisely control the number of antigens fixed to one polymer bead, since the magnetic signal is proportional to the total number of the antigens fixed to the total polymer beads. If the total number of the antigens is same, we obtain the same magnetic signal even when the number of antigens fixed to each polymer bead is scattered.

4. Experimental Results

4.1 Detection of Biotin-Coated Polymer Beads

In order to confirm the validity of the present method, we first detected biotin-coated polymer beads in suspension. In the present experiment, antigens and the detecting antibodies shown in Fig. 6(a) are biotins and avidins, respectively. The magnetic markers couple to the polymer bead through the binding reaction between biotin and avidin.

In the experiment, biotin-coated polystyrene particles with diameter of $d_p = 3.3\,\mu$m (Spherotech Inc., USA) were used. The original polymer beads were diluted to change the concentration, and were put into a reaction cell containing 10 mM phosphate buffer (pH = 7.4) solution. Then, $2\,\mu$g of magnetic markers made of avidin-coated magnetic particles were added. Total volume of the sample was $30\,\mu$l, and diameter of the reaction cell was 5 mm. After 15 min. reaction time, some of the markers couple to the polymer beads, while others remain free, as shown in Fig. 6(a).

The signal from the bound markers was detected with the experimental procedure shown in Fig. 6(b), where the excitation field was $\mu_0 H = 42$ mT, and the waiting time was $T_w = 1$ s. In Fig. 7(a), the experimental result is shown. The horizontal axis is the number N_p of the polymer beads, while the vertical axis represents the signal flux Φ_s detected with the SQUID. As shown, the signal flux increased almost linearly with the number of the polymer beads. This result indicates the validity of the present method, i.e., we can detect only the bound marker even in the presence of the free markers.

Noise signal from the free markers was measured without adding the polymer bead, i.e., for the case of $N_p = 0$. We obtained the noise signal of 0.4 mΦ_0, which gives the minimum detectable signal from the bound markers.

For reference, magnetic relaxation of the bound markers is shown in Fig. 7(b). In the experiment, decay of the signal flux Φ_s was measured after the field $\mu_0 H = 42$ mT

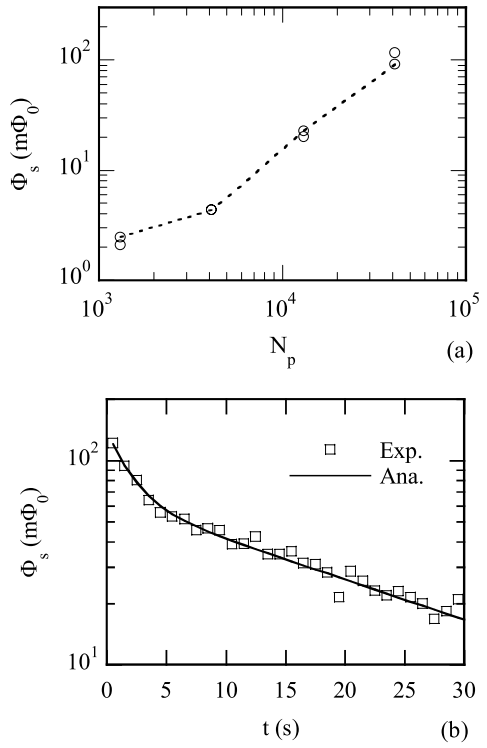

Fig. 7 Detection of biotin-coated polymer beads with the liquid phase immunoassay. (a) Relationship between the signal flux Φ_s and the number N_p of the polymer beds. The broken line is for eyes. (b) Relaxation of the magnetic signal from the bound markers. The solid line shows the calculated result.

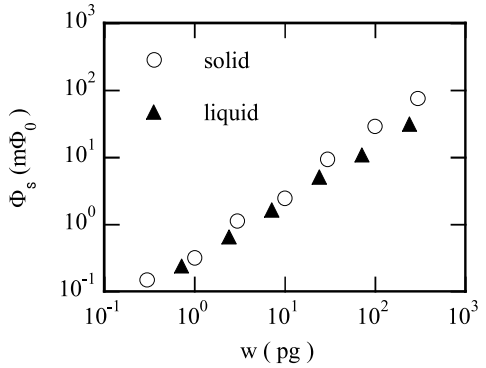

Fig. 8 Detection of IgE. Closed symbols show the experimental results obtained with the liquid phase immunoassay. Open symbols show the results obtained with the conventional solid phase immunoassays, whose procedure is shown in Fig. 5.

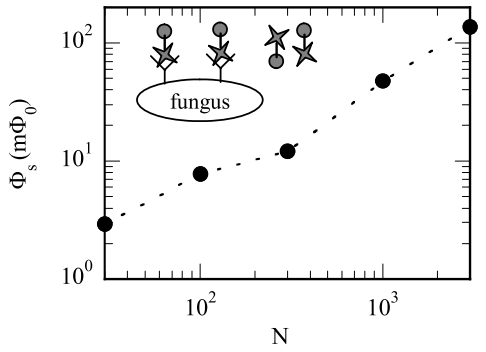

Fig. 9 Detection of *Candida albicans* with the liquid phase immunoassay. Relationship between the number N of *Candida albicans* and the detected signal is shown. The broken line is for eyes.

was removed. As shown in Fig. 7(b), the signal decreased exponentially with time. Comparing the experimental result with Eq. (4), we obtain $(M_i, \tau_{Ni}) = (75, 1.9\,\mathrm{s})$ and $(65, 22\,\mathrm{s})$. The long relaxation time $\tau = 22\,\mathrm{s}$ roughly agrees with the Brownian relaxation time of the polymer beads $\tau_{Bp} = 14\,\mathrm{s}$. On the other hand, the short relaxation time $\tau = 1.9\,\mathrm{s}$ reasonably agrees with the Neel relaxation time $\tau_{N1} = 3.8\,\mathrm{s}$ of the magnetic marker shown in Fig. 4.

4.2 Detection of IgE

Next, we detected protein called IgE. In this experiment, polymer bead coated with capturing antibody called A116UN was used. First, serially diluted IgE was added to the solution containing the polymer beads. Next, the detecting antibody conjugated by the biotin was added. Finally, the avidin-coated magnetic marker was added. The markers are bound to the targets through the biotin-avidin connection. After finishing the binding reaction, we obtain the sample as shown schematically in Fig. 6(a).

Then, we measured the magnetic signal from the bound markers using the experimental procedure shown in Fig. 6(b). The experimental result is shown in Fig. 8 by closed triangles. The horizontal axis is the amount of IgE, while the vertical axis represents the signal flux Φ_s. As shown, almost linear relationship was obtained between the signal flux and the amount of IgE.

For reference, open circles in Fig. 8 show the experimental results obtained with the conventional solid phase immunoassay [18], whose procedure is shown in Fig. 5. We can see that both results agree well with each other. This agreement indicates that the liquid phase immunoassay using the present detection technique is performed correctly.

4.3 Detection of *Candida albicans*

Finally, we show the detection of the fungus called *Candida albicans* [19]. The size of the fungus is typically $4\,\mu$m. In this experiment, we don't use the polymer beads, but the detection antibodies conjugated by the biotin, i.e., Anti-*C. albicans* antibody, was directly coupled to the *Candida albicans*. Then, the magnetic markers conjugated by the avidin were added. After finishing the binding reaction, we obtain the sample as shown schematically in the inset of Fig. 9.

Then, we measured the magnetic signal from the bound markers using the experimental procedure shown in Fig. 6(b). The experimental result is shown in Fig. 9 by closed symbols. The horizontal axis is the number N of the *Candida albicans*, while the vertical axis represents the signal flux Φ_s. As shown, the detected signal Φ_s increased almost proportionally to the number N of the fungus. The

value of $\Phi_s = 2.4\,\mathrm{m}\Phi_o$ was obtained for $N = 30$. Since the noise of the SQUID system was about $0.4\,\mathrm{m}\Phi_0$, we can expect to detect the fungus as small as $N = 5$.

5. Conclusion

We show the detection of biological targets using magnetic marker and SQUID. In this method, detection can be done in the liquid phase, i.e., we can detect only the bound markers even in the presence of unbound (free) markers without using the BF separation process. Since the present method is based on the difference in the magnetic relaxations between the free and bound markers, we clarified them, i.e., the Brownian relaxation of the free markers and the Neel relaxation of the bound markers. Based on these results, we setup the detection system. Usefulness of the present method is demonstrated from the detection of the biological targets, such as biotin-coated polymer beads, IgE and *Candida albicans.*

Acknowledgments

Financial supports by the Japanese Grant-in aid for scientific research (B) is acknowledged.

References

[1] M. Lu, F. Ibraimi, D. Kriz, and K. Kriz, "A combination of magnetic permeability detection with nanometer-scaled superparamagnetic tracer and its application for one-step detection of human urinary albumin in undiluted urine," Biosensors and Bioelectronics, vol.21, no.12, pp.2248–2254, June 2006.

[2] M. Meyer, M. Stehr, S. Bhuju, H. Krause, M. Hartmann, P. Miethe, M. Singh, and M. Keusgen, "Magnetic biosensor for the detection of Yersinia pesos," J. Microbiological Methods, vol.68, no.2, pp.218–224, Feb. 2007.

[3] J. Lange, R. Kötitz, A. Haller, L. Trahms, W. Semmler, and W. Weitschies, "Magnetorelaxometry — A new binding specific detection method based on magnetic nanoparticles," J. Magn. Magn. Mater., vol.252, no.1-3, pp.381–383, Nov. 2002.

[4] H. Grossman, W. Myers, V. Vreeland, R. Bruehl, M. Alper, C. Bertozzi, and J. Clarke, "Detection of bacteria in suspension by using a superconducting quantum interference device," Proc. National Acad. Sciences of U.S.A., vol.101, no.1, pp.129–134, Jan. 2004.

[5] A.P. Astalan, F. Ahrentorp, C. Johansson, K. Larsson, and A. Krozer, "Biomolecular reactions studied using changes in Brownian rotation dynamics of magnetic particles," Biosensors and Bioelectronics, vol.19, no.8, pp.945–951, March 2004.

[6] S.H. Chung, A. Hoffmann, K. Guslienko, S.D. Bader, C. Liu, B. Kay, L. Makowski, and L. Chen, "Biological sensing with magnetic nanoparticles using Brownian relaxation (invited)," J. Appl. Phys., vol.97, no.10, 10R101, May 2005.

[7] G. Glöckl, V. Brinkmeier, K. Aurich, E. Romanus, P. Weber, and W. Weitschies, "Development of by time-dependent a liquid phase immunoassay measurements of the transient magneto-optical birefringence using functionalized magnetic nanoparticles," J. Magn. Magn. Mater., vol.289, pp.480–483, March 2005.

[8] D. Eberbeck, F. Wiekhorst, U. Steinhoff, and L. Trahms, "Aggregation behaviour of magnetic nanoparticle suspensions investigated by magnetorelaxometry," J. Phys. Condensed Matter, vol.18, no.38, pp.S2829–S2846, Sept. 2006.

[9] C.Y. Hong, C.C. Wu, Y.C. Chiu, S.Y. Yang, H.E. Horng, and H.C. Yang, "Magnetic susceptibility reduction method for magnetically labeled immunoassay," Appl. Phys. Lett., vol.88, no.21, 212512, May 2006.

[10] K. Enpuku, K. Soejima, T. Nishimoto, H. Tokumitsu, H. Kuma, N. Hamasaki, and K. Yoshinaga, "Liquid phase immunoassay utilizing magnetic marker and high T-c superconducting quantum interference device," J. Appl. Phys., vol.100, no.5, 054701, Sept. 2006.

[11] K. Enpuku, K. Soejima, T. Nishimoto, T. Matsuda, H. Tokumitsu, T. Tanaka, K. Yoshinaga, H. Kuma, and N. Hamasaki, "Biological immunoassays without bound/free separation utilizing magnetic marker and HTS SQUID," IEEE Trans. Appl. Supercond., vol.17, no.2, pp.816–819, June 2007.

[12] B. Payet, D. Vincent, L. Delaunary, and G. Noyel, "Influence of particle size distribution on the initial susceptibility of magnetic fluids in the Brown relaxation range," J. Magn. Magn. Mater., vol.186, no.1-2, pp.168–174, July 1998.

[13] M. Stromberg, K. Gunnarsson, S. Valizadeh, P. Svedlindh, and M. Stromme, "Aging phenomena in ferrofluids suitable for magnetic biosensor applications," J. Appl. Phys., vol.101, no.2, 023911, Jan. 2007.

[14] B. Fischer, B. Huke, M. Lucke, and R. Hempelmann, "Brownian relaxation of magnetic colloids," J. Magn. Magn. Mater., vol.289, pp.74–77, March 2005.

[15] D.V. Berkov, P. Görnert, N. Buske, C. Gansau, J. Müller, M. Giersig, W. Neumann, and D. Su, "New method for the determination of the particle magnetic moment distribution in a ferrofluid," J. Phys. D: Appl. Phys., vol.33, no.4, pp.331–337, Feb. 2000.

[16] K. Enpuku, T. Tanaka, M. Matsuda, F. Dang, N. Enomoto, J. Hojo, K. Yoshinaga, F. Ludwig, F. Ghaffari, E. Heim, and M. Schilling, "Properties of magnetic nanoparticles in the Brownian relaxation range for liquid phase immunoassays," J. Appl. Phys., vol.102, no.5, 054901, Sept. 2007.

[17] A. Tsukamoto, K. Saitoh, D. Suzki, N. Sugita, Y. Seki, A. Kandori, K. Tsukada, Y. Sugiura, S. Hamaoka, H. Kuma, N. Hamasaki, and K. Enpuku, "Development of multisample biological immunoassay system using HTS SQUID and magnetic nanoparticles," IEEE Trans. Appl. Supercond., vol.15, no.2, pp.656–659, June 2005.

[18] K. Enpuku, K. Inoue, K. Soejima, K. Yoshinaga, H. Kuma, and N. Hamasaki, "Magnetic immunoassays utilizing magnetic markers and a high-T-C SQUID," IEEE Trans. Appl. Supercond., vol.15, no.2, pp.660–663, June 2005.

[19] K. Enpuku, T. Tanaka, T. Matsuda, H. Kuma, N. Hamasaki, F. Dang, N. Enomoto, J. Hojo, K. Yoshinaga, F. Ludwig, F. Ghaffari, E. Heim, and M. Schilling, "Liquid phase immunoassay using magnetic markers and superconducting quantum interference device," Jpn. J. Appl. Phys., vol.46, no.11, pp.7524–7529, Nov. 2007.

Keiji Enpuku received the B.S., M.S. and Dr.Eng. Degrees from Kyushu University in 1976, 1978 and 1981, respectively. He is a Professor in the Research Institute of Superconductor Science and Systems, Kyushu University. He has been engaged in the superconducting electronics. His current interest is the development of high performance high T_c SQUID magnetometer and its applications. Dr. Enpuku is a member of Japan Society of Applied Physics.

Yuki Sugimoto received the B.S. degree from Kyushu University in 2007, and is now master course student of Graduate School of Information Science and Electrical Engineering, Kyushu University. He has been engaged in the development of SQUID system for biological immunoassays.

Yuya Tamai received the B.S. degree from Kyushu University in 2008, and is now master course student of Graduate School of Information Science and Electrical Engineering, Kyushu University. His research theme is the characterization and biological application of magnetic nanoparticles.

Akira Tsukamoto received the B.S. degree from Kyushu University, in 1987 and the Ph.D. degree from Tokyo Institute of Technology, in 2000. In 1987, he joined Central Research Laboratory, Hitachi Ltd., Tokyo, Japan, and engaged in thin film growth of oxide superconductors. He had been on secondment to the Superconductivity Research Laboratory (SRL-ISTEC), Tokyo, Japan, from 1994 to 1997. Since 1997, he joined Advanced Research Laboratory, Hitachi Ltd., where he has been engaged in the research of high T_c superconducting electronics such as SQUID and their fabrication process. Dr. Tsukamoto is a member of the Japan Society of Applied Physics.

Takako Mizoguchi received the V.M.D. and M.S. degrees in Veterinary Medicine from Nihon University in 1995. In 2001, she joined Life Science Group, Hitachi Ltd., Japan, and engaged in the research of full length human cDNA sequencing of national project. Since 2007, she joined Advanced Research Laboratory, Hitachi Ltd., where she has been engaged in the research of magnetic sensor system in clinical laboratory medicine.

Akihiko Kandori received the B.S., M.S. degrees in electrical engineering from Sophia University, Tokyo, in 1988 and 1990 respectively. In 1990, he joined the Central Research Laboratory of the Hitachi Ltd. From 1992 to 1994, he joined the Superconducting Sensor Laboratory of national project. He has been interested in SQUID sensor and application for many years. He received the Ph.D. in Engineer from Sophia University, Tokyo in 1997 and Ph.D. in Medicine from Tsukuba University Ibaraki in 2003. His current interests are biomagnetic imaging and SQUID sensor system.

Naoki Usuki received the B.S. and M.S. degrees from Kyushu University in 1997 and 1999, respectively, and Dr. Sci. degree from Kyushu University in 2002. In 2002, he joined Research and Development section, Hitachi Maxell Ltd., Tokyo, Japan, and engaged in the research of synthesis for inorganic particles.

Hisao Kanzaki received the B.S. degree from Osaka Prefecture University in 1985. In 1985, he joined Kyoto Research Laboratory of Hitachi Maxell Ltd., and engaged in research of magnetic and phosphor particles. His current interests is nanoelectronics using inorganic ultra fine particles.

Kohji Yoshinaga received B.Eng. degree in 1971 and M.Eng. in 1973 from Kumamoto University, and D.Eng. in 1985 form Osaka University. He is a professor of Department of Applied Chemistry, Kyushu Institute of Technology. His research has been focused on functionalization of inorganic ultrafine particles by polymer modification.

Yoshinori Sugiura received the B.S. and M.S. degrees from Shinshu University in 1990 and 1992, respectively. He has engaged in engineering part of plastic products division, INOAC Corporation.

Hiroyuki Kuma received the B.S. and M.S. degrees from Fukuoka University in 1993 and 1995, respectively and Ph.D. degree from Kyushu University in 1999. He is an assistant professor of Faculty of Pharmaceutical Sciences, Nagasaki International University. His current interest is the development of new methods of Clinical Chemistry and Laboratory Medicine.

Naotaka Hamasaki received the M.D. and Ph.D. degrees from Kyushu University in 1968 and 1972, respectively. He was a Professor in the Department of Clinical Chemistry and Laboratory Medicine, Kyushu University and the Director of the Department of Clinical Chemistry and Laboratory Medicine in Kyushu University Hospital. From 2006, he is a professor of Faculty of Pharmaceutical Sciences, Nagasaki International University. He has been engaged in protein chemistry, red blood cell functional regulation, enzymology, clinical chemistry and clinical laboratory medicine. Dr. Hamasaki is the President of Japan Society of Clinical Chemistry (2003–2006), an editorial board of the Clinical Biochemistry (the official journal of Canadian Clinical Chemists) and a member of the Scientific Advisory Committee for the International Congress of Clinical Chemistry.